A CONTRIBUTION TO THE NEPHELOMETRY AND TURBIDIMETRY OF COARSE DISPERSIONS

Antonín TOCKSTEIN and František SKOPAL

Department of Physical Chemistry,
Institute of Chemical Technology, 532 10 Pardubice

Received November 12th, 1986

It was found that the flow of light Φ_r scattered by a dispersion at the angle of 90°, integrated along the optical path of the incoming beam, exhibits an extremum in dependence on the dispersion concentration; its concentration coordinate is a linear function on the dimension of the dispersed particles. This linear dependence is also valid for the concentration corresponding to the selected transparence level on the dependence of the flow Φ_t of light transmitted by the dispersion. A physical model was constructed and the derived equations of the $\Phi_r(C)$ and $\Phi_t(C)$ dependences are in very good agreement with experiments in a concentration range of roughly three orders. The method can be practically applied in determinations of dispersed particle size.

In systems where the optical density (product of turbidity and optical path length) is less than c. 0·2, light scattering is usually described[1] on the assumption of independent particle behaviour, and scattering by a single particle by means of the Mie theory[2,3], so that the concentration dependence of turbidity is a function of the first power of concentration[4]. The dependence on the ratio x of particle size and wavelength and on the ratio m of particle and medium refractive indices is rather complicated and has been tabulated[5]. For $x \to 0$ it leads to Rayleigh scattering (proportionality to square of particle volume), for sufficiently large x turbidity is proportional to particle surface[6] and the system obeys geometrical optics[7,8].

In systems with optical densities exceeding 0·2, multiple scattering occurs, presenting a very difficult theoretical problem. A number of papers have been devoted to its solution[9-11], but the results have not been satisfactory. The expressions obtained were too complicated for practical applications[1]. Therefore at higher dispersion concentrations, experimental procedures were selected so as to prevent multiple scattering (very short optical path[12-14], suitable refractive index of the medium[15,16], optical fibres[17,18]). Recently the problem of multiple scattering has been treated by means of integral equations, but in practical applications iterative procedures had to be used[19].

These studies concentrated mainly on relations between scattered light, its angular dependence and particle size. The concentration dependence was assumed to be linear in first approximation, or a few members of a power series were considered[20], but in analytical applications a calibration curve was generally used. Attenuation along the optical path was taken into account for the incoming beam up to the scattering point[20], but not for the scattered beam. Under such conditions the obtained dependences of scattered light flow densities on particle concentration were monotonous. Only in several cases, where a sufficiently wide concentration range of the dispersed phase was used, extrema appeared[22,23] on the curves of the concentration dependence of scattered light flow density, but these were not subjected to detailed analysis.

The aim of this work is to show that with coarse dispersions ($l \geqq 0{\cdot}5$ μm), usually (starting from concentrations 10^{-3} mol dm^{-3}) representing systems with multiple scattering, the concentration dependence of the flow density of light scattered at an angle of 90° and integrated along the cell passes through a maximum, and that on the basis of a very simple physical model it may be described by a simple equation valid in the concentration range of several orders; this also makes possible a simple particle size determination, without the application of special experimental procedures eliminating multiple scattering.

THEORETICAL

Let us consider a statistically homogeneous monodisperse system with particle concentration C_n, with n designating the degree of aggregation, obeying the relation $C_n \,.\, n = C$, where C is the overall molar concentration given by the mass of the studied compound in 1 dm^3. By interaction with the dispersed particles, the light flow Φ is attenuated, while the overall turbidity $\tau = HC_n = H_rC_n + H_aC_n$ can be decomposed into components corresponding to scattering and absorption.

Light of initial light flow density φ^0 entering the cell by a slit of area s (Fig. 1) reaches a place at distance x from the cell entrance attenuated to $\Phi(x) = \varphi^0 s \,.\, \exp . \,.\, (-C_nHx)$. By the particles contained in the elementary volume $s \,.\, dx$ in this place it is partly absorbed $\Phi_a(x) = \Phi(x) \,.\, dx \,.\, C_nH_a$, partly primarily scattered uniformly in all directions $\Phi_r(x) = \Phi(x) \,.\, dx \,.\, C_nH_r$. For simplicity let us consider only six elementary directions, into each of which the light flow $\Phi_r(x)/6$ is primarily scattered. Along the whole optical path length L, the sum of flow into all directions of the primarily scattered light and of the absorbed light (*i.e.* $\varphi^0 sC_n(H_a + H_r) \int_0^L \exp .$

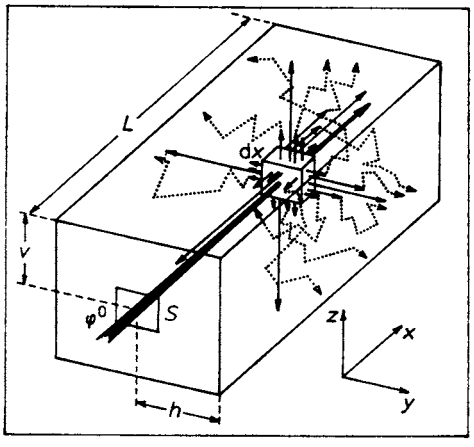

FIG. 1

Scheme of primary and secondary scattering of the incoming beam. Heavy arrow — incoming beam, → primary scattering, ----→ secondary scattering; s area of the entrance slit, v, h, L cell dimensions, φ^0 incoming light flow density

$.(-C_nHx)\,dx)$ together with the light flow $\varphi^0 s \,.\, \exp(-C_nLH)$ that has passed the dispersion without interaction gives the incoming flow $\varphi^0 s$.

Light primarily scattered at the angle of 90° is further attenuated during its progress towards the side wall of the cell, but with much smaller resulting turbidity $\tau_1 = H_1 C_n$, because the place in the side wall (at distance x from the entrance) is reached by other beams from neighbouring places due to secondary scattering. Therefore in place x, the light flow $\Phi_r(x) \,.\, \exp(-C_nH_1h)$ emerges from the side wall at distance h from the axis. By integration over the optical path Lwe obtain for φ_r (for a side wall of surface P_1):

$$\Phi_r = P_1\varphi_r = \varphi^0 s(1 - \exp(-C_nHL)) \,.\, \exp(-C_nH_1h)\,(H_r/6H)\,. \qquad (1a)$$

The dependence $\Phi_r(C_n)$ exhibits a maximum at

$$C_{n,\max} = \ln[1 + HL/(H_1h)]/HL. \qquad (1b)$$

Trough the facing wall (of area P_3) there exits both the light flow $\varphi^0 s \,.\, \exp(-C_nHL)$ that has passed the cell without interactions, and the light flow primarily scattered at all places x at the angle 0° and attenuated along the optical paths $L' - x$ by the turbidity $\tau_2 = H_2C_n$ which may generally differ from τ_1. Thus we obtain

$$\Phi_t = P_3 \,.\, \varphi_t = \varphi^0 s \,.\, \exp(-C_nHL) + (H_r/6) \,.\, \varphi^0 sC_n \,.$$
$$\cdot \int_0^{L'} \exp(-C_nHx) \,.\, \exp[(x - L')\,H_2C_n]\,dx\,, \qquad (2a)$$

so that

$$\Phi_t = \varphi^0 s \left\{ \exp(-C_nHL) + H_r \,.\, \exp(-L'H_2C_n)\, \frac{1 - \exp[-L'(H - H_2)\,C_n]}{6(H - H_2)} \right\}. \qquad (2b)$$

(Note: Due to the broken trajectory, the optical path L' for secondary scattering is generally longer than the optical path of the incoming beam.)

The quantities φ_r and φ_t are not recorded directly by the apparatus, rather the flows $\varphi_r v_r$ and $\varphi_t v_t$ are defined by diaphragms, and these are further electrically amplified at various amplification degrees s_r and s_t to the measured values J_r and J_t. It holds

$$J_r = \varphi_r v_r s_r\,; \quad J_t = \varphi_t v_t s_t \qquad (3a, b)$$

The real concentration of the aggregate C_n is not experimentally accessible and therefore it has to be substituted by the overall concentration C, with $C_n = C/n$. Substituting for φ_r from Eq. (*3a*) into Eq. (*1a*) we obtain the formally three-parameter

function

$$J_r = A_1[1 - \exp(-A_2C)] \,.\, \exp(-A_3C) \qquad (4a)$$

Substituting for φ_t from Eq. (*3b*) into Eq. (*2b*), we obtain the formally five-parameter function

$$J_t = A_0 \,.\, \exp(-A_2C) + A_4 \exp(-A_5C) \,.\, [1 - \exp(-A_6C)] \qquad (4b)$$

By suitably selecting the experimental conditions we may set $A_0 = 100$, thus reducing to four the number of parameters in the expression for J_t.

EXPERIMENTAL

Apparatus

The measurements were performed in a brass tempered attachment of our own construction, connected with the monochromator Specol 10 (Zeiss Jena). Openings for the fitting of photocells (Zeiss Jena) were provided in the centres of the facing and side walls of the attachment. A spiral stirrer (⌀ 10 mm) driven by a 24 V motor (MEZ Náchod) was introduced through the fixed cover of the attachment with a Teflon bearing; the sense of stirring was such as to raise the liquid against gravity. A glass cell of 30 cm^3 volume (ground plan 2 × 3 cm^2) could be introduced through the bottom of the tempered attachment. A beam of monochromatic light (λ 530 nm) entered through a slit (0·4 × 3 mm^2) which could be placed at various levels of the cell. Level values W = 31, 26, 21, 16, and 11 mm (measured from the suspension surface) were used. The flow Φ_t of light transmitted in the direction coaxial with the incoming beam was measured by the photocell on the facing wall. Simultaneously the flow Φ_r of light passing transversally at the angle of 90° was measured by the photocell on the side wall. Both signals were amplified by current amplifiers and lead to a double-trace X–t recorder; the stationary values J_t (in %) and J_r (in scale divisions, as a standard of defined scattering was not available) of both quantities were recorded at all selected concentrations.

At the beginning of the measurement, the electrical parameters were adjusted to a match of the Specol and recorder scales. Dispersions of the desired concentration (mol/dm^3) were prepared by weighing the solid powder into water (with Al_2O_3) or into saturated solution (with the other substances). After thorough shaking in a volumetric flask, 25 cm^3 of the dispersion were introduced into the cell, and after introduction into the attachement, under perfect stirring, the values of the two quantities J_r and J_t were recorded. The measurement was then repeated with another concentration. The concentration range was 1·25 . 10^{-3} to 1 mol/dm^3; temperature 25°C.

Chemicals

Aluminium oxide (corundum) was selected as the model compound, of various particle size as prepared by screening (Treibacher chemische Werke AG, Austria). Fractions of particle diameter l (μm) 5—7, 7—10, 10—15, 15—22, 22—32 were available. The screened fractions with diameters 30—40, 60—80, 80—125, and 160—200 were local products (Carborundum Benátky n. Jiz.). Barium chromate, barium sulphate, and lead sulphate were prepared by mixing of equimolar solutions (0·1 mol/dm^3) of $BaCl_2$ with K_2CrO_4 or Na_2SO_4, and of $Pb(NO_3)_2$ and Na_2SO_4 solutions (all from Lachema Brno); they were filtered and dried after one month of ripening.

Further compounds used were calcium oxide (Lachema Brno) and calcium hydrogen phosphate prepared by mixing of a CaO suspension with an 0·1 mol/dm^3 solution of H_3PO_4 in the stoichiometric ratio. Lead sulphate after drying was screened into two fractions, 0—5 and 5—10 μm. The other products were not fractionated and only the $J_t(C)$ and $J_r(C)$ dependences were followed.

RESULTS AND DISCUSSION

Experiments with corundum as a model compound revealed that the dependence of the quantity J_r (corresponding to the integral flow of scattered transversally transmitted light Φ_r) on the molar concentration C of the suspended substance is a curve which for all fractions exhibits an extremum (Fig. 2) at a position C_{max} on the concentration axis directly proportional to the mean value of the particle dimension l (Fig. 3). The quantity J_t corresponding to the flow of coaxially transmitted light Φ_t changes monotonously with concentration (Fig. 2). It is important that in the coordinates log J_t–log C and log J_r–log C the curves obtained for various fractions can by a suitable shift be brought to mutual coincidence. This is true not only for measurements at each level W, but also for all measurements at various levels W (Fig. 4).

Analogous results were also obtained for lead sulphate. With the other substances where various fractions have not been available, only the dependences $J_r(C)$ and $J_t(C)$ were measured, exhibiting an analogous course as with corundum.

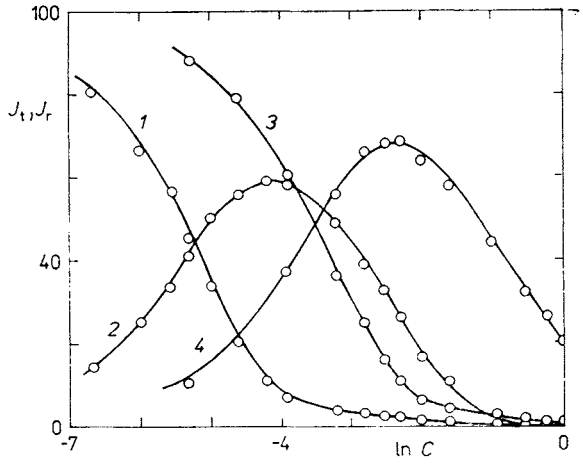

FIG. 2

Flow of transversally (J_r, scale divisions) and coaxially (J_t, %) transmitted light *vs* molar concentration (C, mol/dm^3) at various particle size. *1* and *2* $J_t(C)$ and $J_r(C)$ for fraction l = 5—7 μm, *3* and *4* $J_t(C)$ and $J_r(C)$ for fraction l = 22—32 μm. Full curves calculated according to Eqs (*4a*) and (*4b*), ○ experimental points measured at the level W = 31 mm, 25°C

In Table I the data $J_r(C)$ and $J_t(C)$ measured for the fraction 15–22 μm together with the values calculated according to Eqs. (*4a, b*) are shown for illustration.

The relations for J_r and J_t were tested by nonlinear optimalization using the derivative (Marquard) and nonderivative (simplex) methods. The values A_1 and A_3 obtained from the intercept and slope of the ln J_r–C dependence in the descending branch of the $J_r(C)$ curve, and the coefficient A_2 from the linear dependence ln $\{1 - [J_r \exp(A_3 C)]/A_1\} - C$ were used as starting values; for the other coefficients the following starting values were used: $A_4 = 5$, $A_5 = 0{\cdot}1/C_{max}$, $A_6 = A_2$.

Various fractions were tested at various levels. It appeared that the experimental data are well reproduced by the theoretical relations (see Table I and the full curves in Fig. 2 and 5). Calculations have also shown (Table II) that the dimensionless product $A_i C_{max} = B_i$ and the ratio $J_{r,max}/A_1$ are practically independent of particle size and of level W. In detailed experiments at five levels W with five fractions of linear dimension l, for the quantity J_r linear regression analysis of the product

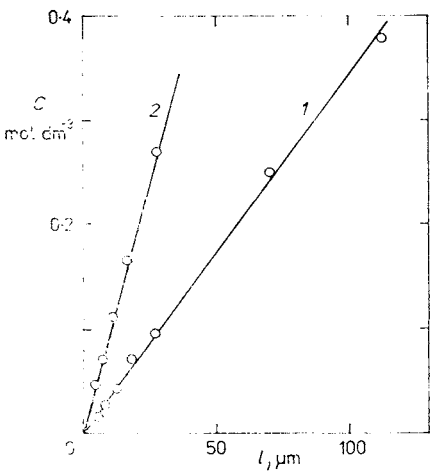

FIG. 3

Dependence of the extremum $C(J_{r,max})$ concentration (mol/dm^3) (curve *1*) and of the concentration $C(J_t = 50)$ (curve *2*) on the mean value of the linear dimension l (μm) of dispersed corundum particles; 25°C

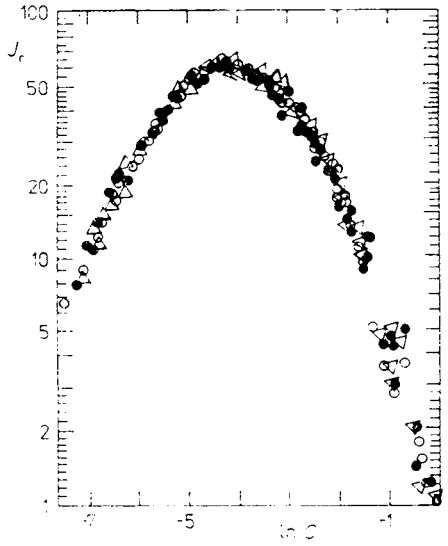

FIG. 4

Coincidence of the log J_r–ln C curves for various fractions and various levels W. Points with equal notation relate to the coincidence log J_r–ln C curves measured for all fractions at equal level W. Points of various notation relate to measurements performed at various levels: ● 11, △ 21, ○ 31 mm; 25°C

values A_2C_{max} was performed in rows (variable W) and columns (variable l); the regression coefficients were zero at the 95% significance level (calculated value $t = 0{\cdot}7-2{\cdot}4$, tabulated $t_{3;0.05} = 3{\cdot}18$) and the A_2C_{max} averages have the same value 3·08. A comparison of the A_2C_{max} and A_3C_{max} products indicates that in agreement with the model, A_2 $[\sim(H_r + H_a)\,L]$ is c. 20 times larger than A_3 $(\sim H_1 h)$.

A confrontation of the experimental data $J_t(C)$ with Eq. (*4b*) revealed (Table III) that the invariance of the A_iC_{max} products holds well for various fractions and agrees with the value following from the curve unification analysis (sixth row of the Table). The value $J_t(C = C_{max})$ calculated for the points where the $J_r(C)$ curves reach their maxima, is also constant within a small scatter and indicates that the mutual position of the $J_t(C)$ and $J_r(C)$ curves remains constant for various fractions.

The parameters A_2 should be equal for the $J_t(C)$ and $J_r(C)$ dependences. For $W = 31$ mm, $J_r(C)$ data and equation (*4a*) yield 3·07, $J_t(C)$ data and equation (*4b*) yield 2·62. Within the proposed simple model this may be regarded as good agreement. The situation is similar for other levels W (see Tables I and II).

In view of the constancy of the B_i values, the relations for J_r and J_t for a given substance (irrespective of particle size and place of measurement) can be written by

TABLE I

$J_r(C)$ and $J_t(C)$ data for the fraction 15—22 μm, $W = 31$ mm

$C \cdot 10^2$ mol/dm^3	J_r[a]		J_t[b]	
	exp.	calc.	exp.	calc.
0·25	6·5	7·1	90·7	91·7
0·5	12·4	13·5	84·0	84·1
0·75	20·0	19·1	73·5	77·2
1	24·0	24·2	70·5	70·8
1·5	32·0	32·6	62·0	59·7
2	40·0	39·2	51·0	50·5
4	56·1	53·8	27·0	26·3
6	59·1	58·3	13·0	14·5
8	61·0	58·5	8·0	8·7
10	57·3	57·0	5·2	5·8
15	52·5	51·4	4·0	3·4
20	42·0	45·8	3·5	2·7
40	27·2	28·7	1·5	1·8
60	19·0	18·0	1·1	1·2
80	13·2	11·3	0·8	0·8
100	9·4	7·1	0·3	0·5

[a] In scale devisions; [b] in %.

means of generally valid B_i coefficients and reduced variables $C/C_{max} = \bar{x}$, $J_r/J_{r,max} = y$, or $J_t/100 = z$ in the form $y = f(\bar{x})$, or $z = g(\bar{x})$, *i.e.* by a single equation for the considered quantity J_r or J_t. In other words, various curves obtained for various fractions and plotted in the coordinates J_r/A_1 or J_t *vs* log C can be brought to coincidence by a shift along the C axis. This enables us to describe the measured data by a single curve. With the $J_r(C)$ data, the calculation procedure was such as to first obtain the group parameters A_i, C_{max}, $J_{r,max}$ for each fraction, and then the set of all data for all fractions (at a given level W) was obtained with the variables $\bar{x}$ and y. From this set of 75 points the overall parameters B_i were obtained (unification

TABLE II

Optimalized parameter values for various fractions and levels of the $J_r(C)$ dependence with Eq. (*4a*)

l μm	J_{rmax}/A_1	A_2C_{max}	A_3C_{max}	$C_{max} \cdot 10^2$ mol/dm^3	J_{rmax} [a]	Number of points
			$W = 11$ mm			
5—7	0·82	3·08	0·15	1·34	56·87	18
7—10	0·86	3·46	0·11	2·16	54·67	14
10—15	0·83	3·12	0·14	3·64	61·33	14
15—22	0·80	2·90	0·17	6·59	57·61	16
22—32	0·84	3·23	0·13	7·58	67·82	13
Unification	0·83	3·13	0·14	1($\bar{x}_m$)	1(y_m)	75
			$W = 21$ mm			
5—7	0·81	3·00	0·16	1·62	58·06	18
7—10	0·86	3·40	0·12	2·65	56·58	14
10—15	0·81	2·97	0·16	4·50	64·25	14
15—22	0·80	2·90	0·17	7·51	59·98	16
22—32	0·83	3·15	0·14	9·87	66·83	13
Unification	0·82	3·07	0·15	0·99	1·01	75
			$W = 31$ mm			
5—7	0·81	2·97	0·16	1·61	58·75	18
7—10	0·85	3·33	0·12	2·53	57·35	14
10—15	0·82	3·04	0·15	4·36	63·51	14
15—22	0·80	2·93	0·17	7·09	58·68	16
22—32	0·83	3·14	0·14	9·63	67·55	13
Unification	0·82	3·07	0·15	0·99	1	75

[a] Expressed in scale divisions.

row in Table I), while for this overall set $\bar{x}_{max} = 1$, $y_{max} = 1$ must hold. For the level $W = 31$ mm this set of experimental data together with the curve calculated according to Eqs (*4a*) and (*4b*) is shown in Fig. 5 and exhibits very good agreement of the equation with experiment in a range of roughly three orders.

For the set of $J_t(C)$ data, equal values of the variable $\bar{x}$ were used, with the corresponding z values serving as the other variable. Besides the parameters B_i, the value of $J_t(C_{max})$ was calculated for various fractions; this value must be invariant when the J_r/A_1–ln C and J_t–ln C curves of various fractions can be brought to

TABLE III

Values of the optimalized parameters for various fractions and $W = 31$ mm of the $J_t(C)$ dependence with Eq. (*4b*) as a four-parameter function

l μm	A_2C_{max}	A_6C_{max}	A_4 %	A_5C_{max}	$C_{max} \cdot 10^2$ mol/dm^3	$J_p(C_{max})$ %	Number of points
5—7	2·65	2·72	4·73	0·12	1·62	11·00	18
7—10	2·67	2·79	4·94	0·13	2·53	10·99	16
10—15	2·83	2·89	6·19	0·19	4·36	10·77	14
15—22	2·58	2·98	3·94	0·14	7·09	10·84	16
22—32	2·62	2·91	5·88	0·16	9·63	12·03	13
Unification	2·62	2·75	5·09	0·15	1($\bar{x}_m$)	11·37	75

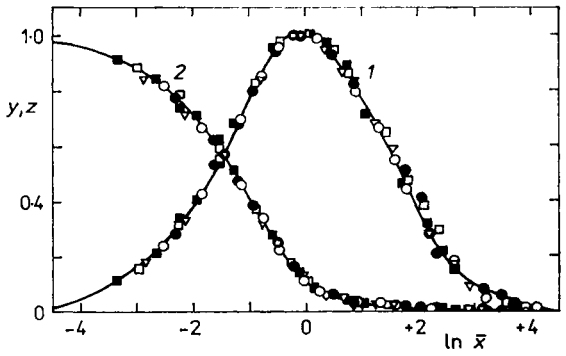

FIG. 5

Unified $y(\bar{x})$ (curve 1) and $z(\bar{x})$ (curve 2) plots for various fractions of Al_2O_3. Full curve calculated according to Eqs (*4a, b*), experimental points for the fractions with l (μm) ○ 5—7, ● 7—10, ▽ 10—15, ■ 15—22, □ 22—32; $W = 31$ mm, 25°C

coincidence. With the four-parameter function (*4b*) (Table III) the group values B_i are in good agreement with the value for the whole set (6th row of the Table).

All these results indicate that the proposed model of light scattering by a disperse system is in good quantitative agreement with the experiments.

The found independence of the B_i coefficients on the size of the dispersed particles follows from Eq. (*1b*) on the assumption that both factors H and H_1 are proportional to the same power of particle dimensions (with large particles proportionality to surface area) and leads to the notion that for the given substance in unit volume there exists a certain critical overall surface area of dispersed particles $Gn^{2/3}C_{n,\max} = K$ (G is a geometrical factor), irrespective of their size, at which maximum flow of transversally transmitted light is attained. Simultaneously the independence of the B_i coefficients of particle size (*i.e.* of n) points to the important fact concerning the linear dependence of $C_{\max}$ on the linear dimensions of the dispersed particles (*i.e.* on $n^{1/3}$). Writing $B_i = A_i C_{\max} = H_{i-2} \cdot C_{\max}/n$ and $H_{i-2} \sim n^{2/3}$, we obtain $C_{\max} \sim n^{1/3}$, in agreement with the experimental dependence.

As for any selected value of J_t, *e.g.* $J_t = 50$, it holds that $C(J_t = 50) = \bar{x}_{50} C_{\max}$ and therefore $C(J_t = 50) = \bar{x}_{50} n^{1/3} K/G$, there exists a linear dependence also beetween the concentration $C(J_t)$ corresponding to the selected J_t level and the linear dimension of particles in various fractions (Fig. 3).

Practically these results can be applied with approximately monodisperse systems for the determination of linear particle dimensions or of their mean values, based on the linear dependence of $C_{\max}$ (with transversally transmitted light), or $C(J_t = 50)$ (with coaxially transmitted light) on l. As the straight lines pass through the origin and are valid even in the range of relatively large particles (200 μm), for the construction of the calibration curves it is sufficient to measure $C_{\max}$ or $C(J_t = 50)$ for one sample where the particle size can be safely determined by screening.

Polydisperse systems will be treated in a subsequent paper.

REFERENCES

1. Oster G.: *Physical Metods of Organic Chemistry*, p. 75. Wiley, New York 1972.
2. Mie G.: Ann. Phys. *25*, 372 (1908).
3. Van der Hulst H. C.: *Light Scattering by Small Particles*, p. 320. Wiley, New York 1957.
4. Meehan E. J., Chiu G.: Anal. Chem. *36*, 536 (1964).
5. Lowan A. N.: *Tables of Scattering Functions for Spherical Particles*. Natl. Bur. Standards, Washington D.C. 1948.
6. Goldberg B.: J. Opt. Soc. Am. *43*, 1221 (1953).
7. Oster G.: *The Science of Moiré Patterns*, p. 30. Barrington, New Jersey 1969.
8. Perrin J. M., Lamy P. L.: Astrophys. Space Sci. Libr. *119*, 245 (1985).
9. Chandrasekhar S.: *Radiative Transfer*. Oxford Univ. Press, Oxford 1950.
10. Kourganoff V.: *Basic Methods in Transfer Problems*, p. 210. Oxford Univ. Press, Oxford 1952.
11. Sobolev V. V.: *Radiative Transfer*, p. 160. van Nostrand, New York 1963.
12. Bauer D. R. in the book: *Polymer Colloids II* (R. M. Fitch, Ed.). Plenum, New York 1980.

13. Bauer D. R.: J. Phys. Chem. *84*, 1592 (1980).
14. Cummins P. G., Staples E. J.: J. Phys., E *14*, 1171 (1981).
15. Kops-Werkhoven M. M., Pathmamanoharan C., Vrij A., Fijnant H. M.: J. Chem. Phys. *77*, 5913 (1982).
16. Pusey P. N., van Mengen W.: J. Phys. *44*, 285 (1983).
17. Tanaka T., Benedek G. B.: Appl. Opt. *14*, 189 (1975).
18. Dyott R. B.: Microwaves Opt. Acoust. *2*, 13 (1978).
19. Dhont J. K. G., De Kruif C. G., Vrij A.: J. Colloid Interface Sci. *105*, 539 (1985).
20. Oster G.: Chem. Rev. *43*, 319 (1948).
21. Wagner P. E.: J. Colloid Interface Sci. *105*, 456 (1985).
22. Candau S. J., Hirsch E., Zana R.: J. Colloid Interface Sci. *105*, 521 (1985).
23. Benoit H., Picot C.: Pure Appl. Chem. *12*, 545 (1966).

Translated by D. Doskočilová.